November 2000

Transgene and Transposon Silencing in *Chlamydomonas reinhardtii* by a DEAH-Box RNA Helicase

Dancia Wu-Scharf
University of Nebraska - Lincoln

Byeong-Ryool Jeong
University of Nebraska - Lincoln, bjeong2@unl.edu

Chaomei Zhang
University of Nebraska - Lincoln

Heriberto D. Cerutti
University of Nebraska - Lincoln, hcerutti1@unl.edu

Transgene and Transposon Silencing in *Chlamydomonas reinhardtii* by a DEAH-Box RNA Helicase

Dancia Wu-Scharf, Byeong-ryool Jeong, Chaomei Zhang, Heriberto Cerutti*

The molecular mechanism(s) responsible for posttranscriptional gene silencing and RNA interference remain poorly understood. We have cloned a gene (*Mut6*) from the unicellular green alga *Chlamydomonas reinhardtii* that is required for the silencing of a transgene and two transposon families. *Mut6* encodes a protein that is highly homologous to RNA helicases of the DEAH-box family. This protein is necessary for the degradation of certain aberrant RNAs, such as improperly processed transcripts, which are often produced by transposons and some transgenes.

In plants (*1*–*5*) and some fungi (*6*, *7*), the overexpression or misexpression of transgenes can induce the silencing of homologous sequences (i.e., transgene and endogenous gene sequences) by a process known as posttranscriptional gene silencing (PTGS). The introduction of double-stranded RNA (dsRNA) triggers a similar phenomenon, called RNA interference (RNAi), in a variety of invertebrate and vertebrate species (*7*–*15*). The widespread occurrence of these phenomena in eukaryotes suggests the involvement of one or more ancestral mechanisms that may have evolved to limit the expression of parasitic elements, such as transposons and viruses (*3*–*8*, *10*). Although several models have been proposed to explain PTGS and RNAi (*1*, *3*, *5*, *7*, *8*, *10*, *13*, *15*), and some genes that are essential for these processes have been identified (*4*–*6*, *8*–*11*), the molecular machinery responsible for RNA recognition and degradation remains largely unexplored.

To gain insight into the molecular mechanism(s) of PTGS, we have screened for mutants defective in this process in *Chlamydomonas reinhardtii*. In *Chlamydomonas*, the *RbcS2::aadA::RbcS2* transgene is silenced at both transcriptional and posttranscriptional levels (*16*, *17*). This transgene is composed of the coding sequence of the eubacterial *aadA* gene (conferring spectinomycin resis-

School of Biological Sciences and Plant Science Initiative, University of Nebraska–Lincoln, E211 Beadle Center, Post Office Box 880666, Lincoln, NE 68588, USA.

*To whom correspondence should be addressed. E-mail: hcerutti1@unl.edu

tance) fused to the regulatory regions of the *Chlamydomonas RbcS2* gene (encoding the small subunit of ribulose-1,5-bisphosphate carboxylase-oxygenase) (*17*). Strain 33-P[300] contains a posttranscriptionally silenced copy of *RbcS2::aadA::RbcS2*. By random insertional mutagenesis (*18*), we isolated a mutant strain (Mut-6) that grew on spectinomycin-containing medium (*19*). Standard genetic analyses confirmed that the gene disrupted in Mut-6 is required for silencing of the transgene (*18*).

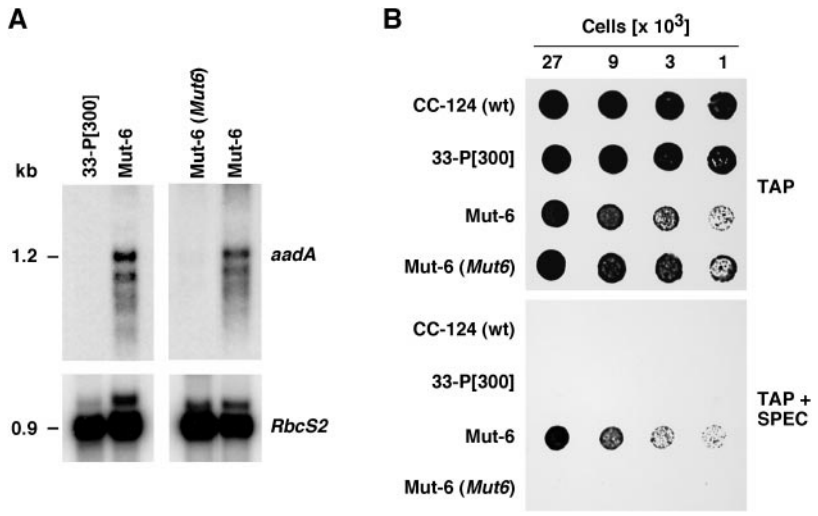

Fig. 1. Expression of the *RbcS2::aadA::RbcS2* transgene is reactivated in Mut-6. (**A**) Northern blot analysis of the silenced strain (33-P[300]), the mutant strain (Mut-6), and the mutant strain complemented with a wild-type copy of *Mut6* [Mut-6(*Mut6*)]. Polyadenylated RNA [poly(A)$^+$ RNA] from the indicated strains was sequentially probed with the coding sequence of *aadA* (upper panels) and with the coding sequence of *RbcS2* (lower panels). (**B**) Growth and survival on tris-acetate-phosphate (TAP) medium or on TAP medium containing spectinomycin (TAP + SPEC) of the indicated strains. CC-124 is the wild-type strain. Cells grown mixotrophically were diluted to the indicated number of cells per 5 μl, spotted on the plates, and incubated for 15 days (*16*).

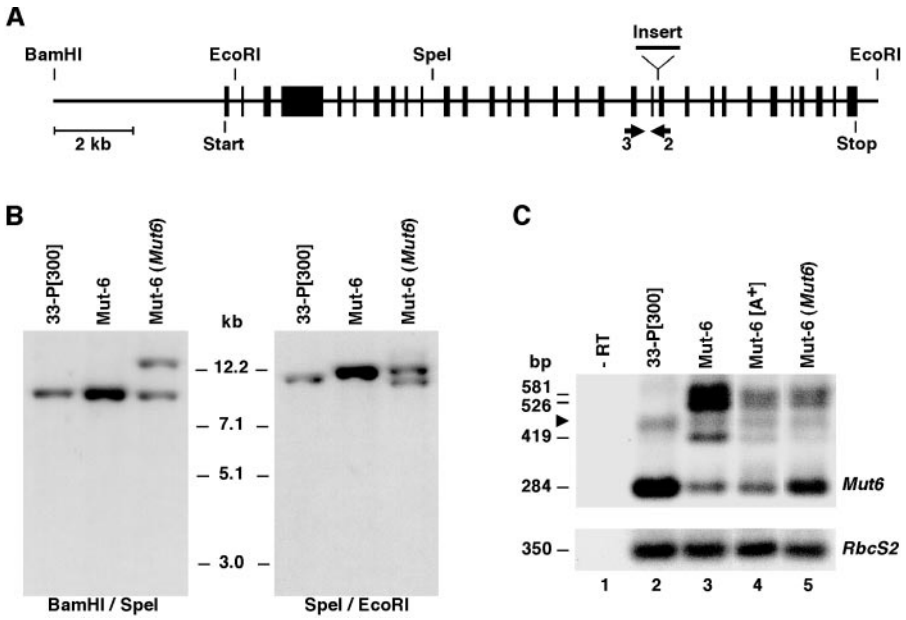

Fig. 2. Structure and expression of *Mut6*. (**A**) Genomic organization of the *Mut6* gene. Exons are indicated as solid boxes. The site of insertion of the tagging plasmid in Mut-6 is shown above the diagram. Specific primers 2 and 3 anneal to exons 21 and 19. (**B**) Southern blot analysis of the indicated strains. Total cell DNA was digested with either Bam HI–Spe I (left panel) or Spe I–Eco RI (right panel) and probed with PCR fragments corresponding to exon 8 or exons 19 through 21, respectively. The Mut-6 lanes were loaded with twice the amount of DNA of the other lanes. (**C**) Analysis of *Mut6* expression by RT-PCR. The upper panel shows a Southern blot of RT-PCR products amplified with *Mut6* primers 2 and 3 (*18*). Amplification of the *RbcS2* mRNA was used as a control for equal amounts of input RNA and for the efficiency of the RT-PCRs (lower panel). Total RNA (lanes 1, 2 , 3, and 5) or poly(A)$^+$ RNA (lane 4) was used as template for RT-PCR (*18*). The input of poly(A)$^+$ RNA was adjusted to obtain an amplification of *RbcS2* equivalent to that in the total RNA samples. A nonspecific RT-PCR fragment is seen across lanes 2 through 5 (upper panel, arrowhead). − RT, no reverse transcriptase.

We next examined the expression of the *RbcS2::aadA::RbcS2* transgene by Northern blot analysis. Hybridization to the *aadA* coding sequence was observed in samples from Mut-6 but was undetectable in those from 33-P[300] (Fig. 1A). The expected size of the *RbcS2::aadA::RbcS2* mRNA is ~1.2 kb, and the smaller transcripts are thought to correspond to improperly processed RNAs that have undergone removal of a cryptic intron, premature termination, and/or incorrect polyadenylation (*17*). Consistent with the steady-state levels of transgenic transcripts, Mut-6 grew on selective medium whereas 33-P[300] could not survive (Fig. 1B). The mutant strain also showed a slower growth rate than the parental strain (Fig. 1B, upper panel). In addition, Mut-6 was moderately sensitive to treatment with two genotoxic agents, methyl methanesulfonate (MMS) and bleomycin, but showed wild-type sensitivity to ultraviolet irradiation (*19*). These pleiotropic phenotypes suggest that *Mut6* plays a role in other cellular processes in addition to transgene silencing.

To clone the *Mut6* gene, we obtained genomic sequences flanking the tagging plasmid (Fig. 2A) by asymmetric polymerase chain reaction (PCR) with nested plasmid primers and an arbitrary degenerate primer. The PCR fragments were used as probes to screen a genomic cosmid library, and one of the isolated cosmids was able to complement the defective phenotypes of Mut-6 (*18*). The complemented strain Mut-6(*Mut6*) was unable to grow on medium containing spectinomycin (Fig. 1B), and the *RbcS2::aadA::RbcS2* transcript was almost undetectable by RNA hybridization (Fig. 1A). In Southern blots of total cell DNA, all strains had a 9.5-kb Bam HI–Spe I fragment, encompassing the 5′ end of *Mut6*. Mut-6(*Mut6*) also showed a larger fragment (Fig. 2B) that resulted from deletion, presumably during integration into the nuclear genome, of cosmid DNA upstream of *Mut6* and digestion within sequences flanking the insertion site (*19*). An 11-kb Spe I–Eco RI fragment, corresponding to the 3′ end of *Mut6*, was restored in the complemented strain. This segment is approximately 1.1 kb larger in Mut-6 because of insertion of the tagging plasmid near the 3′ end of intron 20 (Fig. 2B) (*18*). Thus, Mut-6(*Mut6*) contains one mutant copy of the endogenous *Mut6* gene and one complementing wild-type copy.

We analyzed the expression of *Mut6* by reverse transcriptase PCR (RT-PCR) with primers annealing to exons 19 and 21 (*18*), flanking the site of insertion of the tagging plasmid (Fig. 2A). When total RNA was used

as template, Mut-6 showed a greater than fivefold reduction in the amount of the expected PCR product [a 284–base pair (bp) fragment] when compared with the parental strain (Fig. 2C). It also showed three additional PCR products of 419, 526, and 581 bp (Fig. 2C), containing tagging vector sequences improperly spliced as exons (*18*). These misspliced transcripts were mostly nonpolyadenylated (Fig. 2C; compare Mut-6 with Mut-6[A^+]) and were presumably not translated. Thus, the mutant phenotypes are likely caused by a reduction in the amount of wild-type protein (*18*). The complemented strain partially restored the level of the wild-type PCR product and showed a decrease in the amount of improperly processed transcripts [Fig. 2C; compare Mut-6 and Mut-6(*Mut6*)]. Because Mut-6(*Mut6*) integrated a single copy of *Mut6* without altering the mutant locus (Fig. 2B), these results suggested that the *Mut6* protein might be involved in the degradation of the misprocessed aberrant RNAs.

As observed for several RNAi-resistant mutants in *Caenorhabtidis elegans* (*8*–*10*, *13*), Mut-6 shows elevated transposition activity. We examined the expression of a retrotransposonlike element, *TOC1* (*20*), in the mutant and wild-type strains. The steady-state level of *TOC1* RNA, which is mostly nonpolyadenylated and heterogeneous in size (*20*), is about threefold higher in Mut-6 as compared with the parental and complemented strains (Fig. 3A). The transposition frequency of *TOC1* is accordingly enhanced in Mut-6. We detected no obvious differences in the copies of *TOC1* integrated into the genome of 33-P[300] after 1 year of growth (Fig. 3B; compare 33-P[300]* and 33-P[300]). In contrast, all parallel cultures of the mutant strain showed additional *TOC1* copies (Fig. 3B, arrowheads). The transposition activity of another element that moves via a DNA intermediate, *Gulliver* (*21*), was also higher in Mut-6 (Fig. 3C).

The *Mut6* gene was sequenced entirely from the complementing cosmid clone. The coding sequence was confirmed by RT-PCR with primers designed to anneal to predicted exons (*19*). The deduced *Mut6* protein contains 1431 amino acids and is a member of the DEAH-box RNA helicase family (Fig. 4). Within this family, *Mut6p* is most similar to human PRP16, a homolog of an essential pre-mRNA splicing factor in *Saccharomyces cerevisiae*, and to MOG-1, a gene involved in sex determination in *C. elegans* (*22*) (Fig. 4A). *Mut6p* possesses, in a region spanning residues 751 to 1066, all amino acid motifs that are shared by the DEAH-box family of RNA helicases (*23*) (Fig. 4B). In addition, *Mut6p* has a glycine-rich region spanning residues 150 to 460. This domain includes several RGG repeats (*24*) resembling an RGG box, a motif implicated in RNA binding and protein-protein interactions (*25*). *Mut6p* also has three putative nuclear localization signals and is predicted to be nuclear by both PSORT (a program for detecting sorting signals and predicting subcellular protein localization) and neural network analyses (*26*).

Because *Mut6p* is similar to general splicing factors, we tested whether the mutant strain showed a defect in pre-mRNA splicing. We examined the transcripts of *TubA* (encoding α1 tubulin) and *RbcS2* by both Northern blot hybridization of total RNA and RT-PCR with specific primers. In neither case could we detect unspliced products (*18*), which suggests that *Mut6* is not essential for general splicing. However, Mut-6 showed larger amounts of RNAs corresponding to the *RbcS2::aadA::RbcS2* transgene (Fig. 1A) and to the retroelement *TOC1* (Fig. 3A). It also showed improperly processed *Mut6* transcripts as a result of the tagging plasmid insertion (Fig. 2C). All of these RNAs appeared to be aberrant, with defects in proper processing such as splicing and/or polyadenylation. In the complemented strain, the levels of these RNAs were markedly reduced, suggesting that the *Mut6* RNA helicase might be involved in the degradation of abnormal RNAs. To directly test the role of *Mut6* in the turnover of *TOC1* RNA, transcription was inhibited with actinomycin D and the stability of the retrotransposon transcripts was examined during a 3-hour time course (*18*). In the parental strain, we clearly observed decay of *TOC1* RNA followed by stabilization at the later time points (Fig. 3, D and E). This time course is similar to that reported for short interspersed nuclear elements (SINE) transcribed by RNA

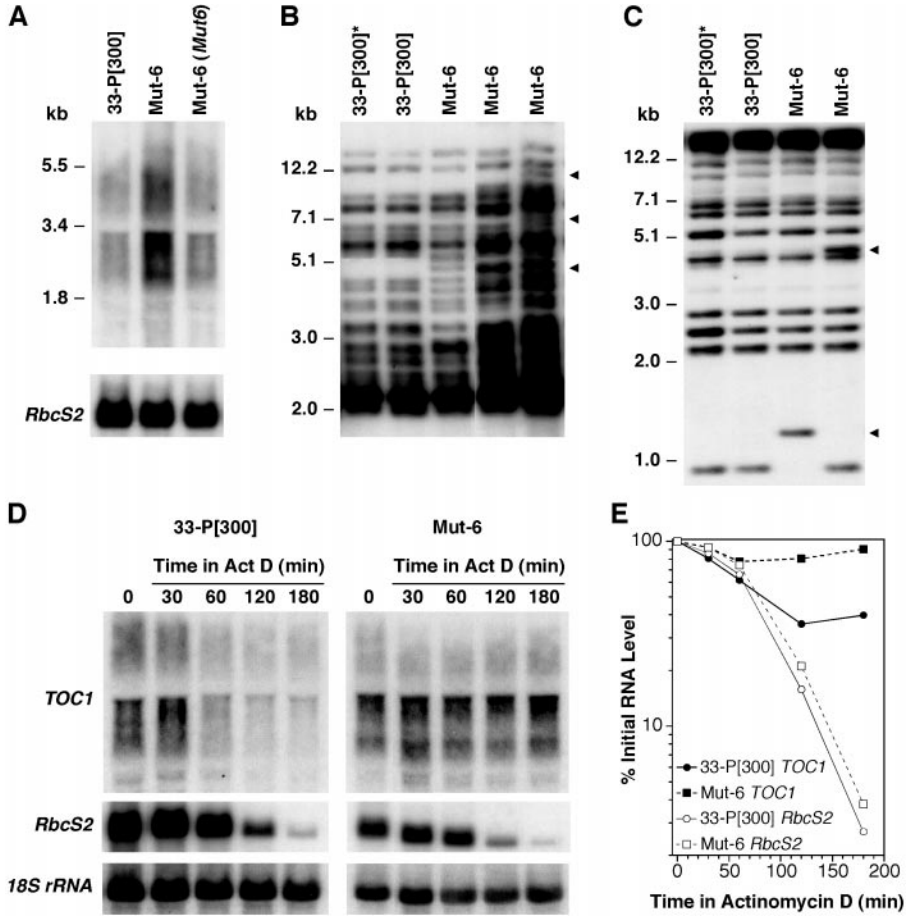

Fig. 3. *Mut6* effects on the activity of a retroelement, *TOC1*, and a DNA transposon, *Gulliver*. (**A**) Northern blot of total RNA probed sequentially for *TOC1* (upper panel) and for *RbcS2* (lower panel). (**B**) Southern blot analysis of *TOC1* transposition. DNA from the silenced strain was isolated and stored frozen (33-P[300]*). Parallel cultures of 33-P[300] and Mut-6 were then grown for 1 year and DNA was isolated again. Total cell DNA was digested with Hinc II and probed for *TOC1*. The arrowheads indicate several new fragments in the subclones of Mut-6. (**C**) Southern blot analysis of *Gulliver* transposition. Parallel cultures of 33-P[300] and Mut-6 were grown as described above. Total cell DNA was digested with Hind III and probed for *Gulliver*. The arrowheads indicate fragments with altered mobility in the subclones of Mut-6. (**D**) Northern blot analysis of RNA decay in 33-P[300] and Mut-6. Total RNA, isolated at the indicated times after the addition of actinomycin D (Act D), was probed sequentially for *TOC1* (upper panel), for *RbcS2* (middle panel), and for 18*S* rRNA (lower panel). Ten micrograms of total RNA were loaded per lane for 33-P[300] and 4 μg of total RNA were loaded per lane for Mut-6. (**E**) Semilog plot of the kinetics of RNA decay after addition of actinomycin D. RNA amounts were determined by phosphorimager analysis of Northern blots, and differences in loading were corrected by normalizing to the levels of 18*S* rRNA. Each time point represents the average of two independent experiments.

polymerase III (*27*). The mutant strain Mut-6 showed a much reduced decay of *TOC1* transcripts, followed by earlier stabilization (Fig. 3, D and E). The initial rate differences in *TOC1* RNA turnover (2.5-fold) are sufficient to account for the different levels of *TOC1* transcripts in 33-P[300] and Mut-6. In contrast, the decay of a correctly processed message, such as *RbcS2*, was virtually identical in the parental and mutant strains (Fig. 3, D and E).

Although *Mut6p* does not appear to function in general splicing (*18*), it could still be involved in the processing of a subset of specific mRNAs whose products are required in various cellular processes. However, the simplest interpretation of our results is that *Mut6p* participates directly in RNA degradation. It could have at least two, not mutually exclusive, roles. (i) *Mut6p* could be a component of the machinery responsible for PTGS and the turnover of homologous RNAs. This process could be induced by dsRNA because antisense transcripts to *TOC1* (*20*) and to *RbcS2::aadA::RbcS2* (*19*) have been detected. (ii) *Mut6p* could be part of an RNA surveillance system that recognizes and degrades improperly processed RNAs. This might explain the sensitivity of Mut-6 to MMS and bleomycin, as *Mut6p* may be necessary to degrade damaged and faulty messages (*28*).

It appears that eukaryotes have evolved a network of mRNA surveillance systems that degrades aberrant RNAs (*29*). These systems might also operate to control the expression of rogue genes encoded by viruses, transposable elements, and some transgenes, because they often produce abnormal RNAs, including antisense RNA and dsRNA (*1*, *3*, *5*, *7*, *8*, *10*). Although dsRNA is the initiator of RNAi, a signal other than dsRNA may be used to detect and suppress transposon activity in *C. elegans* (*13*). RNAs that are not necessarily double-stranded have also been implicated in PTGS in plants (*1*, *3*, *5*, *30*). One possibility is that multisubunit complexes, perhaps analogous to the *S. cerevisiae* exosome (*10*, *31*), degrade a variety of aberrant RNAs and dsRNA-targeted transcripts through the action of different adaptors recognizing specific features of the target RNAs. It is tempting to speculate that the *Chlamydomonas Mut6p* might be involved in such a process.

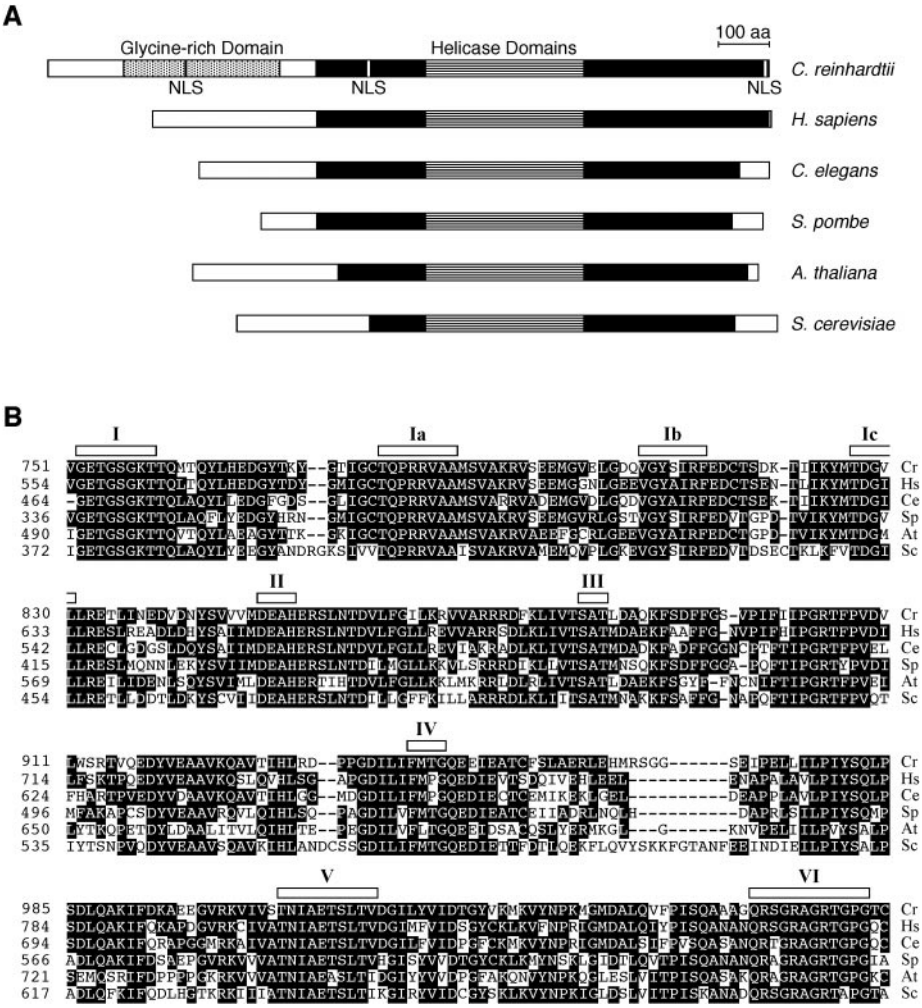

Fig. 4. *Mut6* belongs to the DEAH-box RNA helicase family. (**A**) Schematic representation of *Mut6p* and five closely related DEAH-box RNA helicases. The sequences correspond to hPRP16 (*Homo sapiens*, AAC27431), MOG-1 (*C. elegans*, P34498), a putative pre-mRNA splicing factor (*Schizosaccharomyces pombe*, CAB52799), DDX8 (*Arabidopsis thaliana*, Q38953), and PRP16 (*S. cerevisiae*, NP_013012). The solid areas indicate aligned regions with greater than 45% identity. The helicase domains are shown as horizontally striped boxes. Putative nuclear localization signals (NLS) and a unique glycine-rich domain (shaded box) are indicated in the diagram of *Mut6p*. The coding sequence of *Mut6* has been deposited in GenBank (accession no. AF305070). (**B**) Sequence alignment of the helicase domains of *Mut6p* (Cr) and the five related DEAH-box proteins (Hs, hPRP16; Ce, MOG-1; Sp, *S. pombe* putative splicing factor; At, DDX8; and Sc, PRP16) (*24*). Boxes above the sequences indicate the positions of conserved helicase domains (*23*).

References and Notes

1. R. A. Jorgensen, Q. D. Que, M. Stam, *Trends Genet.* **15**, 11 (1999).
2. A. J. Hamilton, D. C. Baulcombe, *Science* **286**, 950 (1999).
3. J. M. Kooter, M. A. Matzke, P. Meyer, *Trends Plant Sci.* **4**, 340 (1999).
4. P. Mourrain *et al.*, *Cell* **101**, 533 (2000).
5. T. Dalmay, A. Hamilton, S. Rudd, S. Angell, D. Baulcombe, *Cell* **101**, 543 (2000).
6. C. Cogoni, G. Macino, *Science* **286**, 2342 (1999).
7. A. Fire, *Trends Genet.* **15**, 358 (1999).
8. R. F. Ketting, T. H. A. Haverkamp, H. G. A. M. van Luenen, R. H. A. Plasterk, *Cell* **99**, 133 (1999).
9. H. Tabara *et al.*, *Cell* **99**, 123 (1999).
10. J. M. Bosher, M. Labouesse, *Nature Cell Biol.* **2**, E31 (2000).
11. A. Smardon *et al.*, *Curr. Biol.* **10**, 169 (2000).
12. R. F. Ketting, R. H. A. Plasterk, *Nature* **404**, 296 (2000).
13. A. Grishok, H. Tabara, C. C. Mello, *Science* **287**, 2494 (2000).
14. S. M. Hammond, E. Bernstein, D. Beach, G. J. Hannon, *Nature* **404**, 293 (2000).
15. P. D. Zamore, T. Tuschl, P. A. Sharp, D. P. Bartels, *Cell* **101**, 25 (2000).
16. H. Cerutti, A. M. Johnson, N. W. Gillham, J. E. Boynton, *Plant Cell* **9**, 925 (1997).
17. _____, *Genetics* **145**, 97 (1997).
18. For experimental details and supplemental material, see *Science* Online at www.sciencemag.org/feature/data/1051322.shl.
19. D. Wu-Scharf, H. Cerutti, unpublished data.
20. A. Day, J. D. Rochaix, *J. Mol. Biol.* **218**, 273 (1991).
21. P. J. Ferris, *Genetics* **122**, 363 (1989).
22. A. Puoti, J. Kimble, *Mol. Cell. Biol.* **19**, 2189 (1999).
23. E. Jankowsky, A. Jankowsky, *Nucleic Acids Res.* **28**, 333 (2000).
24. Single-letter abbreviations for the amino acid residues are as follows: A, Ala; C, Cys; D, Asp; E, Glu; F, Phe; G, Gly; H, His; I, Ile; K, Lys; L, Leu; M, Met; N, Asn; P, Pro; Q, Gln; R, Arg; S, Ser; T, Thr; V, Val; W, Trp; and Y, Tyr.
25. A. M. Krecic, M. S. Swanson, *Curr. Opin. Cell Biol.* **11**, 363 (1999).
26. K. Nakai, P. Horton, *Trends Biochem. Sci.* **24**, 34 (1999).
27. R. H. Kimura, P. V. Choudary, C. W. Schmidt, *Nucleic Acids Res.* **27**, 3380 (1999).
28. S. M. Hecht, *J. Nat. Prod.* **63**, 158 (2000).
29. P. Hilleren, R. Parker, *Annu. Rev. Genet.* **33**, 229 (1999).
30. M. Metzlaff, M. O'Dell, R. Hellens, R. B. Flavell, *Plant J.* **23**, 63 (2000).
31. C. Allmang *et al.*, *Genes Dev.* **13**, 2148 (1999).

32. We thank J. Kovar and D. Weeks for making available plasmid pJK7 and an anonymous reviewer for helpful suggestions. Supported by grants to H.C. from NSF (grant number MCB-9808473) and from the Nebraska Research Initiative.

13 April 2000; accepted 13 September 2000